Eur. Phys. J. A **25**, s01, 305–310 (2005)
DOI: 10.1140/epjad/i2005-06-035-y

EPJ A direct
electronic only

Cluster structure in stable and unstable nuclei

Y. Kanada-En'yo[1,a,b], M. Kimura[2,b], and H. Horiuchi[3]

[1] Institute of Particle and Nuclear Studies, High Energy Accelerator Research Organization, 1-1 Oho, Tsukuba, Ibaraki 305-0801, Japan
[2] Institute of Physical and Chemical Research (RIKEN), Saitama 351-0198, Japan
[3] Department of Physics, Kyoto University, Kitashirakawa-Oiwake, Sakyo-ku, Kyoto 606-01, Japan

Received: 24 September 2004 /
Published online: 25 April 2005 –

Abstract. Cluster structure in stable and unstable nuclei has been studied. We report recent developments of theoretical studies on cluster aspect, which is essential for structure study of light unstable nuclei. We discuss negative-parity bands in even-even Be and Ne isotopes and show the importance of cluster aspect. Three-body cluster structure and cluster crystallization are also introduced. It was found that the coexistence of cluster and mean-field aspect brings a variety of structures to unstable nuclei.

PACS. 21.60.-n Nuclear structure models and methods – 23.20.Lv γ transitions and level energies

1 Introduction

Clustering is one of the essential features in nuclear dynamics. As already known, cluster structures appear in light stable nuclei such as ^{8}Be, ^{12}C and ^{20}Ne. Owing to recent developments of experimental and theoretical studies on unstable nuclei, cluster structures have been found also in light unstable nuclei. For instance, cluster states have been suggested in neutron-rich Be isotopes [1,2,3,4,5,6,7,8,9,10,11,12,13,14]. Furthermore, in the heavier nuclei, the importance of cluster aspect are found in such phenomena as molecular resonances, which has been observed in stable *sd*-shell and *pf*-shell nuclei. On the other hand, we should remind the reader that the mean-field nature is the other essential aspect. It is important that the coexistence of these two natures, the cluster and the mean-field aspects brings a variety of structure to unstable nuclei as well as stable nuclei.

We can see the coexistence of cluster and mean-field aspects in such stable nuclei as ^{12}C, where the 3α-cluster structure plays an important role. The ground state is considered to contain the 3α-cluster *and* $p_{3/2}$ sub-shell closure configurations [15]. In the excited states above the 3α threshold energy, developed 3α-cluster structures are expected. The 0^+_2, 0^+_3 and 2^+_1 states of ^{12}C have been discussed in relation to the 3α structure for a long time [16,17,15,18,19].

In unstable nuclei, a variety of cluster structure appears, and the coexistence of cluster and mean-field aspects becomes further important. In halo nuclei, ^{6}He and ^{11}Li, the behavior of valence neutrons is described by a hybrid configuration of the independent single-particle motion *and* di-neutron structure [20,21,22,23,24,25]. The former is a kind of mean-field nature, and the latter is regarded as cluster aspect. In the neutron-rich Be isotopes, a molecular-orbital picture describes well the structure of low-lying states [4,5,9,26]. 2α core and valence neutron structure are found in many low-lying states of neutron-rich Be. The molecular orbitals are formed in the mean-field of 2α-cluster system, and the valence neutrons are moving in the molecular orbitals around the 2α core. It means that a kind of mean-field nature is seen in the valence neutron behavior, and simultaneously the 2α-cluster core plays an important role to form the mean-field for the molecular orbitals. In the highly excited states of ^{12}Be, molecular resonant states with ^{6}He clusters have been suggested [12,13,14].

As mentioned above, a variety of structure has been revealed and it motivates one to extend theoretical frameworks. In these years, the development of theoretical framework for cluster structure has been remarkable following the progress of physics of unstable nuclei. Such cluster models as core+neutrons models and multi-cluster models have been applied to unstable nuclei. These models are useful to describe the details of the relative motion between clusters and motion between core and valence neutrons. In addition to simple cluster models based on two-body or three-body calculations, extended models such as stochastic variational method (SVM) [6,10,20,27], molecular orbital method (MO) [4,5,9,28] and generator coordinate method (GCM) [24,29,30,31] have been developed for structure study of unstable nuclei. We

[a] Conference presenter;
e-mail: yenyo@yukawa.kyoto-u.ac.jp
[b] *Present address*: Yukawa Institute for Theoretical Physics, Kitashirakawa Oikawe-Cho, Kyoto 606-8502, Japan.

should give a comment on another important development of cluster models concerning studies of resonances in loosely bound systems. The complex scaling method (CSM) [21,22,25,32,33], method of analytic continuation in the coupling constant (ACCC) [34], and R-matrix theory [35] were applied to estimate widths of the resonances in cluster models.

In most of cluster models, the existence of clusters is *a priori* assumed. However, the assumption of clusters is not necessarily valid for systematic study of unstable nuclei. Instead, it is important to take into account degrees of all single nucleons. In this sense, a method of antisymmetrized molecular dynamics (AMD) [15,36,37,38] is one of the powerful approaches which do not rely on the model assumption of cluster cores. The wave function of the AMD is similar to the Bloch-Brink model, but is based completely on single nucleons. Namely, an AMD wave function is given by a Slater determinant of single-particle Gaussian wave functions, where all the centers of Gaussians are independent variational parameters. Therefore, the degrees of all single-nucleon wave functions are independently treated. Due to the flexibility of the AMD wave function, it can describe various cluster states as well as shell-model-like states. Similar model space has been adopted in a method of Fermionic molecular dynamics (FMD) [39]. One of the remarkable advantages of the recent version of FMD is that the effect of tensor force is incorporated based on realistic nuclear forces in this framework [40], while phenomenological effective nuclear forces are usually used in other cluster models.

Owing to the progress of calculations with these models, the structure study of stable and unstable nuclei has been now extended to a wide mass number region up to sd- and pf-shell region, and it reveals the importance of cluster aspect in ground and excited states of various nuclei. In this paper, we take some topics on cluster aspect in unstable nuclei. In the next sect. 2, we focus on the negative-parity bands in even-even nuclei. The excited states of Be and Ne isotopes are discussed in relation to cluster structure. In sect. 3, we report 3α structure in C isotopes and discuss the mechanism of rigid cluster structure. Finally, we give a summary in sect. 4.

2 Negative-parity bands in even-even nuclei

As well known, ^{20}Ne has a ^{16}O+α-cluster structure, which was confirmed by parity doublets, $K^\pi = 0^+_1$ and $K^\pi = 0^-_1$ rotational bands. The parity doublets arise from the reflection asymmetry of the intrinsic state, which is caused by $^{16}\mathrm{O}+\alpha$ clustering. Thus, negative-parity bands can be good probes for cluster structure. It is interesting that another type of negative-parity rotational band with cluster structure appears in neutron-rich nuclei based on single-particle excitation of neutron orbitals. In such a state, the origin of the negative parity is the single-particle excitation. A typical example is the $1p$-$1h$ excitation of the valence neutron orbitals in the molecular orbital states. The negative-parity bands with the $1p$-$1h$ excitation have been suggested in low-lying states of neutron-rich Be isotopes.

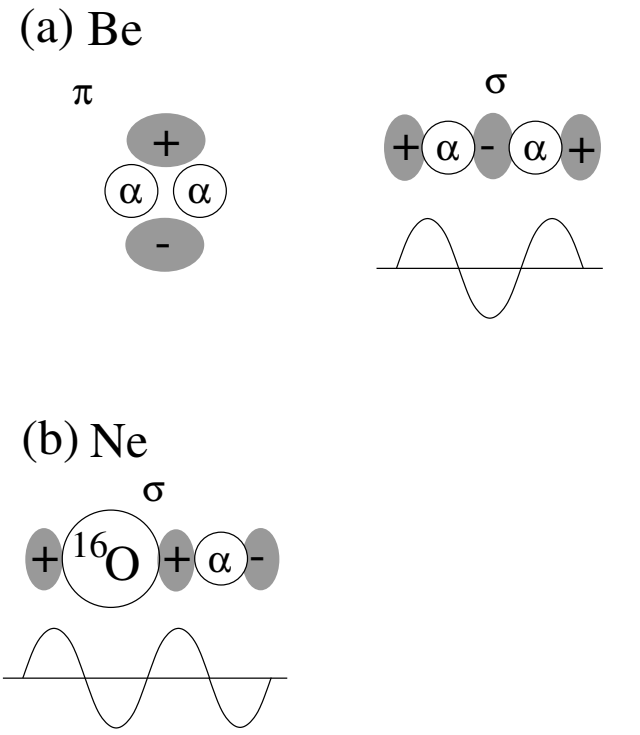

Fig. 1. Schematic figure of the molecular orbitals: the π- and σ-orbitals around 2α core (a) and σ-orbital around $^{16}\mathrm{O}+\alpha$ core (b).

One of the characteristics of those negative-parity bands is the quanta $K^\pi = 1^-$, which differs from the $K^\pi = 0^-$ of the parity doublets. In this section, we discuss the negative-parity bands in neutron-rich Be and Ne isotopes.

2.1 Be isotopes

The low-lying states of neutron-rich Be isotopes are well described by the molecular orbital picture based on the 2α core and valence neutron structure. In the 2α system, the molecular orbitals are formed by a linear combination of p-orbits around the 2α core. In neutron-rich Be, the valence neutrons occupy the molecular orbitals. The negative-parity orbitals are called as "π-orbitals" and the longitudinal orbital with positive parity is a "σ-orbital" (fig. 1). As a result of the formation of molecular orbitals in Be isotopes, a negative-parity $K^\pi = 1^-$ band is constructed because of the one valence-neutron excitation of the molecular orbitals in the rotating cluster structure. In ^{10}Be, the $K^\pi = 1^-$ band is regarded as such a molecular-orbital band with the one-neutron excitation, which can be described by a $\pi^1\sigma^1$ configuration in the molecular-orbital picture [5,8,9,26].

In ^{12}Be, many rotational bands are theoretically suggested. Figure 2 shows the energy levels of ^{12}Be calculated by variation after spin-parity projection in the AMD framework. The energy variation is performed for the J^π eigenstates projected from a single-Slater AMD wave function. For the k-th J^π state, the wave function is obtained

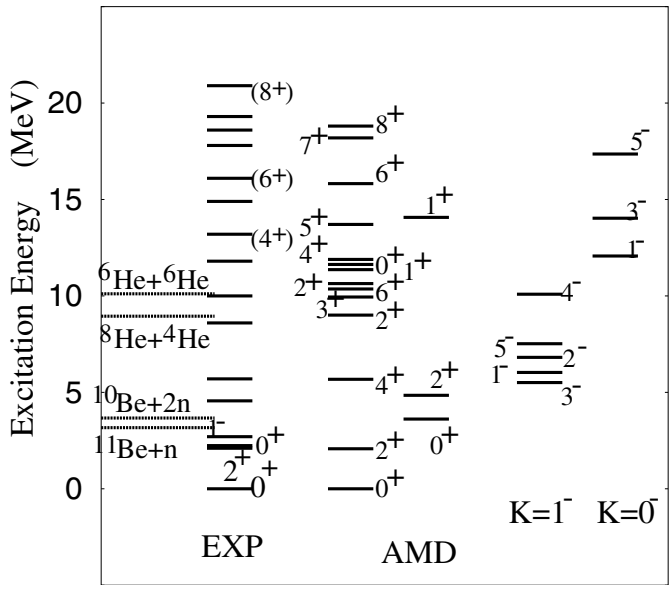

Fig. 2. Energy levels of ^{12}Be. The MV1 case 1 force ($m = 0.65$) + G3RS ($u_{ls} = 3700\,\mathrm{MeV}$) force is adopted. The details of the AMD calculations are explained in [12].

by the energy variation for the component orthogonal to the lower $J^\pi_1, \cdots, J^\pi_{k-1}$ states. The energy variation is performed by a frictional cooling method (a imaginary time method). After the variation, we superpose the 22 AMD wave functions of ^{12}Be determined by the variation for various spin and parity to obtain better wave functions. The adopted effective nuclear force is the MV1 (Modified Volkov) force [41], which contains a zero-range three-body repulsive term in addition to the two-range two-body central force, complemented by a two-range spin-orbit force of G3RS [42] and Coulomb force. The details of the framework and calculations are given in [12] and references therein. The theoretical results obtained by the AMD calculations agree well to the experimental data. We found three positive-parity rotational bands $K^\pi = 0^+_1, 0^+_2$ and 0^+_3. The ground band consists of the intruder states ($2\hbar\omega$ excited configurations), which are well-deformed states with the 2α core and the surrounding neutrons. On the other hand, the normal neutron-shell-closed states belong to the $K^\pi = 0^+_2$ band. It means that the breaking of neutron magic number $N = 8$ occurs in ^{12}Be. In the $K^\pi = 0^+_3$ band, ^{6}He + ^{6}He molecule-like states are predicted in the results. The experimentally measured 4^+ and 6^+ states are the candidates of these molecular resonant states.

Next, let us analyze the negative-parity states of ^{12}Be. In the negative-parity states, two bands $K^\pi = 1^-$ and $K^\pi = 0^-$ are obtained by the AMD calculations. The lower one is the $K^\pi = 1^-$ band which consists of 1^-, 2^-, 3^-, 4^- and 5^- states. These states are the molecular-orbital states, which can be described by the $\pi^3\sigma^1$ (three neutrons in the π-orbitals and one neutron in the σ-orbital) configuration of the valence neutrons in the 2α-cluster system. This $K^\pi = 1^-$ band is consistent with the molecular-orbital band predicted by von Oertzen *et al.* [26]. On the other hand, we also obtain the higher negative-parity band ($K^\pi = 0^-$). The $K^\pi = 0^-$ band is formed by a parity asymmetric neutron structure of the ^{4}He + ^{8}He-like intrinsic state. This band is associated with the well-known parity doublet $K^\pi = 0^-$ band in ^{20}Ne. Descouvemont and Baye performed GCM calculations of ^{12}Be [30], where ^{6}He + ^{6}He and ^{4}He + ^{8}He configurations are coupled and the relative distance between two He clusters is chosen as the generator coordinate. The effective two-body nucleon-nucleon interaction was chosen as the Volkov V2 force [43] ($m = 0.45$, $b = -h = -0.2374$) + zero-range spin-orbit force ($S_0 = 30\,\mathrm{MeV\,fm^5}$) + Coulomb. These interaction parameters are chosen so as to reproduce the ^{6}He + ^{6}He and ^{4}He + ^{8}He thresholds simultaneously. In the GCM calculations, they found the $K^\pi = 0^-$ band with the ^{8}He + α-like cluster structure, which is consistent with the higher negative-parity band ($K^\pi = 0^-$) found in the AMD results. It is concluded that the existence of two negative-parity bands $K^\pi = 1^-$ and 0^- is suggested in ^{12}Be. The $K^\pi = 1^-$ band is the molecular orbital band, while the $K^\pi = 0^-$ band is the parity doublet caused by the parity asymmetric intrinsic state. Both bands have developed cluster structure, however, there exists a remarkable difference between these two bands concerning the origin of negative parity. In the $K^\pi = 1^-$ band, the negative parity originates from the one-particle excitation of the valence neutron in the molecular orbitals. On the other hand, the negative parity of the $K^\pi = 0^-$ band arises from the parity asymmetric shape of the intrinsic state. Due to the collectivity, the $E1$ transition into the ground state is stronger as $B(E1; 0^+_1 \to 1^-_2) = 1.0\,\mathrm{e^2fm^4}$ from the $K^\pi = 0^-$ band than $B(E1; 0^+_1 \to 1^-_1) = 0.2\,\mathrm{e^2fm^4}$ from the $K^\pi = 1^-$ band. It is interesting that the lower one is the molecular-orbital $K^\pi = 1^-$ band which has a kind of mean-field nature in the valence neutron behavior. We consider that the experimentally observed $K^\pi = 1^-$ state [44] corresponds to the band-head state of the $K^\pi = 1^-$ band.

2.2 Ne isotopes

In analogy to neutron-rich Be isotopes, von Oertzen proposed molecular orbital structure of Ne isotopes based on the ^{16}O + α-cluster core [26]. In the molecular-orbital picture, the cluster structure may develop when the valence neutrons occupy the molecular σ-orbitals, which correspond to longitudinal fp-like orbits (fig. 1). In ^{22}Ne, they proposed a developed cluster structure where two valence neutrons occupy the σ orbit. As a result of the development of cluster, the parity doublet $K^\pi = 0^-$ band arise from the parity asymmetric structure of the ^{16}O + α-cluster core. We performed the AMD + GCM calculations of ^{22}Ne with Gogny D1S force. The deformed-base AMD wave functions are used, and the constraint on the oscillator quanta of the deformed harmonic oscillator is applied in addition to the constraint on the deformation parameter β. We find that the parity doublet $K^\pi = 0^+$ and 0^- bands arise from the developed ^{16}O + α core with two valence neutrons in the σ-like orbital in the excited states

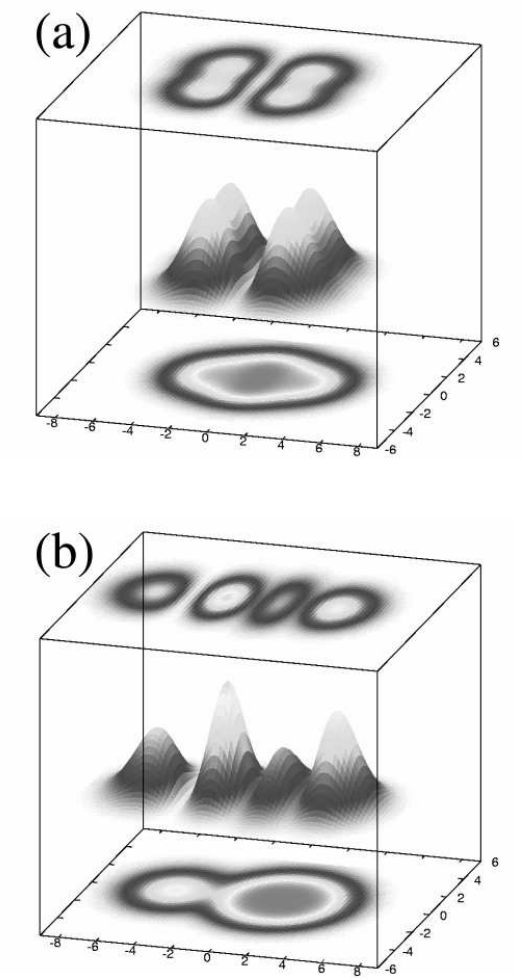

Fig. 3. Density distribution of ^{22}Ne. The density of the intrinsic states of the ground band is illustrated in panel (a). Panel (b) shows the density in the $K^\pi = 0^-$ band with valence neutrons in longitudinal σ-like orbitals. The middle and top figures in each box show the density distribution of the single-neutron wave functions of the highest single-particle level. The matter density of the total system is displayed at the bottom of the box.

below the $^{18}\mathrm{O} + \alpha$ threshold energy. In fig. 3(b), we show the developed $^{16}\mathrm{O} + \alpha$ cluster and the single-particle orbit of the last valence neutron, which is consistent with the molecular σ-orbital around the $^{16}\mathrm{O} + \alpha$ core (fig. 1(b)). The details of the AMD calculations of ^{22}Ne will be published in a future paper.

Recently, Rogachev *et al.* observed the α-cluster states in negative-parity bands which start from the 1^- state at 12 MeV excitation energy of ^{22}Ne [45]. These negative-parity states above the $^{18}\mathrm{O} + \alpha$ threshold energy can be associated with the developed $^{18}\mathrm{O} + \alpha$-cluster structure. The microscopic calculations of the excited states of ^{22}Ne were performed by Dufour and Descouvemont by using the GCM method within a $^{18}\mathrm{O} + \alpha$-cluster model [46]. They chose the inter-cluster distance as the generator coordinate, and incoorporated many $^{18}\mathrm{O}+\alpha$ channels by defining the ^{18}O internal wave functions in the s, p, and sd shell-model configurations. The effective interaction was chosen as the Volkov V2 force ($m = 0.6259$) + zero-range spin-orbit force ($S_0 = 30\,\mathrm{MeV\,fm^5}$) + Coulomb. The negative-parity bands with the developed $^{18}\mathrm{O} + \alpha$-cluster states are found in the results of the GCM calculations. These negative-parity states in the parity doublet band exist in the energy region above $^{18}\mathrm{O}+\alpha$ threshold energy (9.7 MeV excitation energy of ^{22}Ne), which is consistent with the observed α-cluster states [45]. These theoretical and experimental works suggest that the $^{18}\mathrm{O} + \alpha$-cluster bands appear above the $^{18}\mathrm{O} + \alpha$ threshold, while the molecular-orbital bands with the developed $^{16}\mathrm{O} + \alpha$ cluster and two neutrons in the molecular σ-orbital may exist in the lower-energy region than the $^{18}\mathrm{O} + \alpha$-cluster bands.

Next, we discuss a further neutron-rich nucleus, ^{30}Ne. The AMD+GCM calculations of ^{30}Ne with the deformed-base AMD wave functions [38,47] have been performed by Kimura *et al.* [47] The deformation parameter β was chosen as the generator coordinate. As is usually done in the GCM calculations of Hartree-Fock (HF) framework, the AMD wave functions obtained by the variation with the constraint on the β value were projected to the spin-parity eigenstates, and were superposed. The effective nuclear interaction was chosen as the Gogny D1S force [48] and Coulomb. In the results, many low-lying bands have been predicted. They found that the ground band of ^{30}Ne is dominated by $2\hbar\omega$ configuration, which indicates the breaking of magic number $N = 20$. The results suggest $4\hbar\omega$ state with a $4p$-$4h$ neutron configuration appear in the low-lying 0_3^+ band (the excitation energy $E_x(0_3^+) = 4\,\mathrm{MeV}$). The $4p$-$4h$ state has a parity asymmetric proton structure which indicates the developed $^{16}\mathrm{O}+\alpha$-cluster core. One of the striking results is the prediction of a low-lying $K^\pi = 1^-$ band with a $3p$-$3h$ neutron configuration. The structure of the $K^\pi = 1^-$ band is described by the excitation of neutrons in the deformed mean field. The excitation energy of the band-head 1^- state of the $K^\pi = 1^-$ band is predicted to be less than 3 MeV. It is surprising that such many-particle many-hole states may exist in low-energy region of ^{30}Ne. These results indicate the softness of neutron $N = 20$ shell, and point the importance of neutron excitation in the deformed mean-field in neutron-rich nuclei.

3 Three-center clustering and cluster crystallization

As mentioned before, the 3α-cluster structure is known in ^{12}C. The 3α-cluster states with a triangular shape and linear-chain structure have been discussed for a long time. Recently, Tohsaki *et al.* proposed a gas-like dilute 3α state and succeeded to describe the properties of the 0_2^+ state of ^{12}C with Bose-condensed wave functions of 3 α-particles. In the experimental side, the broad resonances at 10 MeV are recently assigned to be 0_3^+ and 2_2^+ states, which are candidates of 3α-cluster states.

In neutron-rich C isotopes, three-center cluster structures with the 3α-cluster core are expected to exist

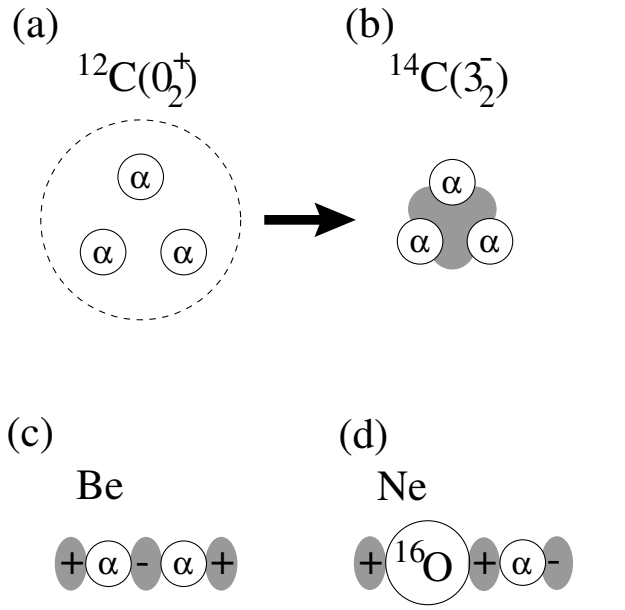

Fig. 4. Schematic figures for cluster structure in $^{12}C(0_2^+)$ (a), $^{14}C(3_2^-)$ (b), neutron-rich Be with the molecular σ-orbitals (c), neutron-rich Ne with the σ-orbitals (d).

in the excited states. Possible linear chain structures were suggested to appear in highly excited states of ^{16}C and ^{15}C [26,49,50]. In ^{14}C, Itagaki *et al.* proposed an equilateral-triangular shape with 3α core in $K^\pi = 3^-$ band which is stabilized by excess neutrons [51]. They performed molecular orbital model calculations of ^{14}C with 3α and excess neutrons. In the model, the molecular orbitals around the 3α core are introduced, and the excess two neutrons occupy them. With respect to the positions of 3α clusters and configurations of the valence neutrons, the spin-parity projected wave functions are superposed by the diagonalization of Hamiltonian as is done in the GCM method. The Volkov V2 force complemented by a two-range spin-orbit force of G3RS were used in the calculation of ^{14}C. In their calculations, it was found that the excess neutrons distribute in the gap space between α cores. As a result, the triangular configuration of 3α is stabilized, and the $K^\pi = 3^-$ rotational band is formed due to the D_{3h} symmetry. It should be noticed that the neutron configuration in the orbital given by the linear combination of the molecular orbitals on the α-α bonds is important in the $K^\pi = 3^-$ band. The experimentally observed 3_2^-, 4_1^- and 5_1^- states are the candidates of the members of this $K^\pi = 3^-$ band. Comparing the gas-like 3α structure in the 0_2^+ of ^{12}C, the triangular shape of the 3α becomes more rigid due to the valence neutrons in ^{14}C. Itagaki *et al.* named this phenomenon as "α crystallization".

The mechanism of rigid cluster structure is understood as follows. In case of ^{12}C, 3α clusters are weakly bounded and can move freely in the cluster states above the 3α threshold energy (fig. 4(a)). When two neutrons are added into those 3α states, the valence neutrons move around the α cores and occupy the gap space between α cores (see fig. 4(b)). As a result, the α clusters cannot freely move because the motion of the α clusters are forbidden due to the Pauli blocking between the valence neutrons and the neutrons inside the α clusters. Thus, the 3α clusters are crystallized to form the triangular shape in ^{14}C. Itagaki's idea of "cluster crystallization" can be also applied to two-body cluster states as well as the 3α-cluster states. As mentioned before, the developed cluster structures are suggested in neutron-rich Be and Ne isotopes which have $\alpha + \alpha$-cluster and $^{16}O + \alpha$-cluster cores, respectively. Especially, the remarkable enhancement of cluster structure is expected when the valence neutrons occupy the longitudinal molecular orbitals, namely, the σ-orbitals. The σ-orbitals have nodes along the longitudinal axis. It is important that the valence neutrons in σ-orbitals occupy the gap space between the core clusters (fig. 4(c) and (d)). As a result, when the core clusters approach to each other, they feel repulsion against the valence neutrons in the gap region because of Pauli blocking. In other words, due to the existence of the valence neutron in the gap space, the core clusters cannot move so freely and are kept away. Thus, the cluster structure is enhanced.

It is concluded that the valence neutrons in molecular orbitals play important roles in the cluster states of neutron-rich nuclei. The valence neutrons bound the clusters more deeply, and may make the spatial configuration of clusters more rigid.

4 Summary

The recent development of theoretical and experimental studies revealed that the cluster aspect is an essential feature in unstable nuclei as well as stable nuclei. The coexistence of cluster and mean-field aspects brings a variety of structure to unstable nuclei. We reported some topics concerning the cluster structure of unstable nuclei while focusing on the negative-parity bands of even-even nuclei. In the low-lying states of neutron-rich nuclei, the mean-field aspect of the valence neutron behavior is found to be essential. The negative-parity rotational bands appear in the low-energy region due to the particle-hole excitation in the deformed neutron mean-field. On the other hand, in high-energy region, there may exist negative-parity states in the parity doublet bands which are caused by asymmetric intrinsic shapes. In Be and Ne isotopes, developed cluster structures with 2α-cluster and ^{16}O+α-cluster cores were suggested, while 3α-cluster structures were predicted in C isotopes in many theoretical studies. The valence neutrons in the molecular orbitals play an important role to stabilize cluster structure.

The computational calculations in this work were supported by the Supercomputer Projects of High Energy Accelerator Research Organization (KEK). This work was supported by the Japan Society for the Promotion of Science and Grant-in-Aid for Scientific Research of the Japan Ministry of Education, Culture, Sports, Science and Technology.

References

1. A.A. Korsheninnikov *et al.*, Phys. Lett. B **343**, 53 (1995).
2. M. Freer *et al.*, Phys. Rev. Lett. **82**, 1383 (1999); M. Freer *et al.*, Phys. Rev. C **63**, 034301 (2001).
3. A. Saito *et al.*, *Proceedings of the International Symposium on Clustering Aspects of Quantum Many-Body Systems*, edited by A. Ohnishi, N. Itagaki, Y. Kanada-En'yo, K. Kato (World Scientific Publishing Co.) p. 39.
4. M. Seya, M. Kohno, S. Nagata, Prog. Theor. Phys. **65**, 204 (1981).
5. W. von Oertzen, Z. Phys. A **354**, 37 (1996); **357**, 355 (1997).
6. K. Arai, Y. Ogawa, Y. Suzuki, K. Varga, Phys. Rev. C **54**, 132 (1996).
7. A. Doté, H. Horiuchi, Y. Kanada-En'yo, Phys. Rev. C **56**, 1844 (1997).
8. Y. Kanada-En'yo, H. Horiuchi, A. Doté, Phys. Rev. C **60**, 064304 (1999).
9. N. Itagaki, S. Okabe, Phys. Rev. C **61**, 044306 (2000); N. Itagaki, S. Okabe, K. Ikeda, Phys. Rev. C **62**, 034301 (2000).
10. Y. Ogawa, K. Arai, Y. Suzuki, K. Varga, Nucl. Phys. A **673**, 122 (2000).
11. Y. Kanada-En'yo, Phys. Rev. C **66**, 011303 (2002).
12. Y. Kanada-En'yo, H. Horiuchi, Phys. Rev. C **68**, 014319 (2003) and references therein.
13. M. Ito, Y. Sakuragi, Y. Hirabayashi, Phys. Rev. C **63**, 064303 (2001).
14. P. Descouvemont, D. Baye, Phys. Lett. B **505**, 71 (2001).
15. Y. Kanada-En'yo, Phys. Rev. Lett. **81**, 5291 (1998).
16. H. Morinaga, Phys. Rev. **101**, 254 (1956); Phys. Lett. **21**, 78 (1966).
17. Y. Fujiwara, H. Horiuchi, K. Ikeda, M. Kamimura, K. Kato, Y. Suzuki, E. Uegaki, Prog. Theor. Phys. Suppl. **68**, 29 (1980).
18. A. Tohsaki, H. Horiuchi, P. Schuck, G. Röpke, Phys. Rev. Lett. **87**, 192501 (2001).
19. Y. Funaki, A. Tohsaki, H. Horiuchi, P. Schuck, G. Röpke, Phys. Rev. C **67**, 051306 (2003).
20. K. Varga, Y. Suzuki, R.G. Lovas, Nucl. Phys. A **571**, 447 (1994).
21. A. Csótó, Phys. Rev. C **48**, 165 (1993); A. Csótó, Phys. Rev. C **49**, 3035 (1994).
22. S. Aoyama, S. Mukai, K. Kato, K. Ikeda, Prog. Theor. Phys. **93**, 99 (1995).
23. Y. Tosaka, Y. Suzuki, K. Ikeda, Prog. Theor. Phys. **83**, 1140 (1990).
24. P. Descouvemont, Nucl. Phys. A **626**, 647 (1997).
25. S. Aoyama, K. Kato, K. Ikeda, Prog. Theor. Phys. Suppl. **142**, 35 (2001).
26. W. von Oertzen, Nuovo Cimento. A **110**, 895 (1997); W. von Oertzen, Eur. Phys. J. A **11**, 403 (2001).
27. K. Varga, Y. Suzuki, I. Tanihata, Nucl. Phys. A **588**, 157c (1995).
28. S. Okabe, Y. Abe, H. Tanaka, Prog. Theor. Phys. **57**, 866 (1977); S. Okabe, Y. Abe, Prog. Theor. Phys. **59**, 315 (1978); **61**, 1049 (1979).
29. D. Baye, P. Descouvemont, N.K. Timofeyuk, Nucl. Phys. A **577**, 624 (1994).
30. P. Descouvemont, D. Baye, Phys. Lett. B **505**, 71 (2001).
31. P. Descouvemont, Nucl. Phys. A **699**, 463 (2002).
32. A.T. Kruppa, R.G. Lovas, B. Gyarmati, Phys. Rev. C **37**, 383 (1988); A.T. Kruppa, K. Kat, Prog. Theor. Phys. **84**, 1145 (1990).
33. S. Aoyama, K. Kat, K. Ikeda, Phys. Rev. C **55**, 2379 (1997).
34. S. Aoyama, Phys. Rev. C **68**, 034313 (2003).
35. K. Arai, P. Descouvemont, D. Baye, W.N. Catford, Phys. Rev. C **68**, 014310 (2003).
36. Y. Kanada-En'yo, H. Horiuchi, A. Ono, Phys. Rev. C **52**, 628 (1995); Y. Kanada-En'yo, H. Horiuchi, Phys. Rev. C **52**, 647 (1995).
37. Y. Kanada-En'yo, H. Horiuchi, Prog. Theor. Phys. Suppl. **142**, 205 (2001).
38. Y. Kanada-En'yo, M. Kimura, H. Horiuchi, C. R. Phys. **4**, 497 (2003).
39. H. Feldmeier, K. Bieler, J. Schnack, Nucl. Phys. A **586**, 493 (1995).
40. T. Neff, H. Feldmeier, Nucl. Phys. A **713**, 311 (2003).
41. T. Ando, K. Ikeda, A. Tohsaki, Prog. Theor. Phys. **64**, 1608 (1980).
42. N. Yamaguchi, T. Kasahara, S. Nagata, Y. Akaishi, Prog. Theor. Phys. **62**, 1018 (1979); R. Tamagaki, Prog. Theor. Phys. **39**, 91 (1968).
43. A.B. Volkov, Nucl. Phys. **74**, 33 (1965).
44. H. Iwasaki *et al.*, Phys. Lett. B **491**, 8 (2000).
45. G.V. Rogachev *et al.*, Phys. Rev. C **64**, 051302 (2001).
46. M. Dufour, P. Descouvemont, Nucl. Phys. A **738**, 447 (2004).
47. M. Kimura, H. Horiuchi, Prog. Theor. Phys. **111**, 841 (2004).
48. J.F. Berger, M. Girod, D. Gogny, Nucl. Phys. A **428**, 23c (1984).
49. N. Itagaki, S. Okabe, K. Ikeda, I. Tanihata, Phys. Rev. C **64**, 014301 (2001).
50. W. von Oertzen, M. Freer, Y. Kanada-En'yo, submitted to Rev. Mod. Phys.
51. N. Itagaki, T. Otsuka, K. Ikeda, S. Okabe, Phys. Rev. Lett. **92**, 142501 (2004).